Triple oxygen isotope evidence for the pathway of nitrous oxide production in a forested soil with increased emission on rainy days

Weitian Ding[1], Urumu Tsunogai[1], Tianzheng Huang[1], Takashi Sambuichi[1], Wenhua Ruan[1], Masanori Ito [1], Hao Xu[1], Yongwon Kim [2], Fumiko Nakagawa[1]

[1]Graduate School of Environmental Studies, Nagoya University, Furo-cho, Chikusa-ku, Nagoya 464-8601, Japan

[2]International Arctic Research Center, University of Alaska Fairbanks, Fairbanks, Alaska 99775-7320, USA

Corresponding author: Weitian Ding

Email: dwt530754556@gmail.com

Abstract

Continuous increases in atmospheric nitrous oxide (N_2O) concentrations are a global concern. Both nitrification and denitrification are the major pathways of N_2O production in soil, one of the most important sources of tropospheric N_2O. The ^{17}O excess ($\Delta^{17}O$) of N_2O can be a promising signature for identifying the main pathway of N_2O production in soil. However, reports on $\Delta^{17}O$ are limited. Thus, we determined temporal variations in the $\Delta^{17}O$ of N_2O emitted from forested soil for more than one year and that of soil nitrite (NO_2^-), which is a possible source of O atoms in N_2O. We found that N_2O emitted from the soil exhibited significantly higher $\Delta^{17}O$ values on rainy days (+0.12±0.13 ‰) than on fine days (−0.30±0.09 ‰), and the emission flux of N_2O was significantly higher on rainy days (38.8±28.0 μg N m^{-2} h^{-1}) than on fine days (3.8±3.1 μg N m^{-2} h^{-1}). Because the $\Delta^{17}O$ values of N_2O emitted on rainy and fine days were close to those of soil NO_2^- (+0.23±0.12 ‰) and O_2 (−0.44 ‰), we concluded that although nitrification was the main pathway of N_2O production in the soil on fine days, denitrification became active on rainy days, resulting in a significant increase in the emission flux of N_2O. This study reveals that the main pathway of N_2O production can be identified by precisely determining the $\Delta^{17}O$ values of N_2O emission from soil and by comparing the $\Delta^{17}O$ values with those of NO_2^-, O_2, and H_2O in the soil.

1. Introduction

Nitrous oxide (N_2O) is a strong greenhouse gas and an essential substance in stratospheric ozone depletion (Dickinson and Cicerone, 1986). Since pre-industrial times, the atmospheric N_2O level has increased by 24 % to 335.8 ppb, with an average growth rate of 1.05 ppb yr^{-1} in the last decade (WMO, 2023). Terrestrial soils account for ~60 % of total N_2O emissions (Tian et al., 2020). Therefore, better knowledge of the pathways of N_2O production in soils is required to establish mitigation measures.

Both nitrification and denitrification are representative microbial pathways of N_2O production in soils (Wrage et al., 2001). Nitrification is the oxidation of ammonium (NH_4^+) to nitrate (NO_3^-) via aerobic microbial activity, during which N_2O is produced as a byproduct of hydroxylamine (NH_2OH) oxidation to nitrite (NO_2^-), while denitrification is the reduction of NO_3^- to NO_2^- and then to N_2O which is further reduced to nitrogen (N_2) via facultative anaerobes (Figure 1). Soil conditions such as moisture content, O_2 availability (Bateman and Baggs, 2005; Zhu et al., 2013), temperature (Luo et al., 2007), and fertilizer types (Zhu et al., 2013) have been proposed as parameters to determine the pathways of N_2O production in soils.

Techniques such as acetylene blockage (Balderston et al., 1976; Lin et al., 2019), artificial isotope tracers (^{15}N and ^{18}O) (Mulvaney and Kurtz, 1982; Wrage et al., 2004), and natural stable isotopes (Toyoda et al., 2013; Yu et al., 2020) are conventionally used to identify the pathways of N_2O production via nitrification and denitrification. Both acetylene blockage and artificial isotope tracers are mostly performed in laboratory (*in vitro*) incubations because they are costly, complicated, and time-consuming in field research. Natural stable isotopes such as $\delta^{15}N$, $\delta^{18}O$, and SP (^{15}N site preference) can be

设置了格式：上标

used to identify the pathways of N_2O production in soils (Decock and Six, 2013; Toyoda et al., 2017; Verhoeven et al., 2019). However, further reduction of N_2O to N_2 after the production of N_2O until emission from soil to air results in significant changes in the $\delta^{15}N$, $\delta^{18}O$, and SP values of N_2O due to the fractionation of isotopes, which makes the identification process difficult (Ostrom et al., 2007).

Recent studies on the $\Delta^{17}O$ value of NO_3^- (the definition detailed in Section 2.4) have reported that $\Delta^{17}O$ is a useful natural signature for clarifying the complicated biogeochemical processes in terrestrial ecosystems (Ding et al., 2022, 2023, 2024; Michalski et al., 2004; Tsunogai et al., 2010). Although the values of $\delta^{15}N$, $\delta^{18}O$, and SP can vary during various fractionation processes of isotopes within terrestrial ecosystems, the $\Delta^{17}O$ value remains almost stable because possible variations in $\delta^{17}O$ and $\delta^{18}O$ values during the processes of biogeochemical isotope fractionation follow the relation of $\delta^{17}O \approx 0.5\ \delta^{18}O$, which cancels out the variations in the $\Delta^{17}O$ value (Young et al., 2002). Consequently, the mixing of the same oxygen compounds with different $\Delta^{17}O$ values is the primary cause of variations in $\Delta^{17}O$ values throughout the biogeochemical processes in terrestrial ecosystems.

Because N_2O produced through nitrification is a byproduct of the oxidation reaction between NH_4^+ (to NH_2OH) and O_2, the $\Delta^{17}O$ value of N_2O produced through nitrification is expected to be close to that of tropospheric O_2 (Figure 1) (Kool et al., 2007, 2011; Wrage et al., 2005), with previous studies reporting a $\Delta^{17}O$ value of −0.44 ‰ (Sharp and Wostbrock, 2021). Conversely, the $\Delta^{17}O$ value of N_2O produced through denitrification is expected to be close to that of NO_2^- (Figure 1) (Kool et al., 2007, 2011; Wankel et al., 2017; Wrage et al., 2005). Because O atoms in NO_2^- are derived from either soil NO_3^-

($\Delta^{17}O$ = from 0 to +20 ‰) or H_2O ($\Delta^{17}O$ = +0.03±0.01 ‰) (Hattori et al., 2019; Nakagawa et al., 2018; Uechi and Uemura, 2019), significant differences in $\Delta^{17}O$ values between N_2O produced through nitrification and that produced through denitrification are expected if the additional contributions of O atoms derived from soil H_2O are insignificant in N_2O during the processes of N_2O production in soils through nitrification and denitrification (Figure 1) (Kool et al., 2007).

Previous studies have identified the elevated $\Delta^{17}O$ values in atmospheric N_2O ($\Delta^{17}O \approx$ +0.9 ‰), observed in both stratospheric and tropospheric air (Cliff et al., 1999; Kaiser et al., 2003; Thiemens and Trogler, 1991). Komatsu et al. (2008) subsequently conducted the first $\Delta^{17}O$ measurements of N_2O emitted from a soil to assess whether soil N_2O could be the source of high $\Delta^{17}O$ values of atmospheric N_2O. However, the temporal variations of the $\Delta^{17}O$ values for N_2O emitted from soil remain unknown. Besides, whether $\Delta^{17}O$ values of N_2O can be used to identify the pathways of N_2O production in soils has not been discussed. Additionally, the advantages of $\Delta^{17}O$ signature, relative to other natural stable isotopes, for identifying the pathways of N_2O production remain unclear. To address these, in this study, we measured precise $\Delta^{17}O$ values for N_2O emitted from forested soil and those for NO_2^- in the soil. Additionally, we conducted similar observations in the same soil artificially fertilized with Chile saltpeter or urea to investigate the possible contributions of O atoms derived from soil H_2O in N_2O during N_2O production.

删除了: reported
删除了: $\Delta^{17}O$ values for
删除了: in
删除了: air
删除了: However, there have been few reports on $\Delta^{17}O$ values for N_2O emitted from soil (Komatsu et al., 2008). W
删除了: remains unclear
删除了: have not been discussed

2. Methods

2.1 Study site

111 The study site was located in a secondary warm-temperate forest within an urban area
112 (35°10'N, 136°58'E, Figure 2), approximately 50 m from the common building of the
113 Graduate School of Environmental Studies at Nagoya University. The lowest, highest,
114 and mean monthly temperatures recorded at the nearest meteorological station (Nagoya
115 station) were 5.2 ℃ (in January), 28.9 ℃ (in July), and 18.5 ℃, respectively, from April
116 2022 to July 2023. The annual mean precipitation was approximately 1800 mm. The soil
117 stratum in the forested field possessed an approximate depth of 20 cm, characterized by a
118 bulk density of 1.12 g/cm^3. Details of the forest have been described in the previous study
119 (Hiyama et al., 2005).
120
121 **2.2 Sampling of N_2O**
122 Samples of N_2O emitted from the forested soil under natural conditions were collected
123 18 times (n = 18) from April 2022 to July 2023 in a field with an area of 5 m^2 (Figure
124 2b). Among the samples, 12 were collected on fine days, whereas 6 were collected on
125 rainy days. A fine day is defined as a day without precipitation for 48 hours prior to the
126 end of each sampling. The total precipitation within 12 h at the end of each sampling of
127 the rainy days exceeded 12 mm.
128 The sampling of N_2O emitted from the artificially fertilized soil was performed during
129 a period of fine weather in three plots (1 m^2 for each located more than 5 m away from
130 each other) within the same forested field, located approximately 3 m away from the plot
131 where we conducted the sampling under natural conditions (Figures 2b and 2c). Either
132 urea ($CO(NH_2)_2$, 46 % TN) or Chile saltpeter (KNO_3, 14 % TN) was applied to two of
133 the plots (U and CS plots) on 2023/7/16 at the same N amount of 250 kg N ha^{-1}. Urea is a

synthetic N fertilizer (Sun & Hope Ltd., Japan), and Chile saltpeter (SQM Ltd., USA) contains NO_3^- with a high $\Delta^{17}O$ value of +19 ‰ (determined through the internationally distributed isotope reference materials USGS-34 and USGS-35). The third plot was blank, meaning no fertilizer was added (NF plot). Sampling of N_2O from each plot was performed twice on days 2 and 6 after the addition of each fertilizer.

To precisely determine $\Delta^{17}O$ of N_2O, more than 60 nmol of N_2O is required (Komatsu et al., 2008), which corresponds to more than 4 L of air containing N_2O at atmospheric concentrations. Accordingly, in this study, a flow chamber made of polypropylene with dimensions of 0.8 m × 0.3 m × 0.18 m was deployed onto the sampling site throughout each day of sampling (Figure S1). This chamber has an inlet and outlet port with an inner diameter of 1 cm. The outlet port was connected to an air pump using Tygon tubing, and the inlet port was open to ambient air. Using the air pump, the air in the chamber was taken into a 5-L aluminum bag, along with the gases emitted by the soil, as illustrated in Figure S1. The flow rate of the air pump was set at 100 ml/min throughout the deployment of the chamber; thus, each sampling lasted 45 min until 4.5 L of gas was collected into the aluminum bag. Each gas sampling was started 2 h after deployment of the flow chamber; thus, it took more than 8 h to collect four samples. In addition to the gas samples emitted from the soil, ambient air in the forest was sampled into two 3-L vacuum stainless steel canisters (SilcoCan, Restek).

2.3 Sampling and analysis of forested soil

After collecting the gas samples to determine N_2O, a soil sample (approximately 150 g) was randomly collected from more than four places beneath the chamber.

Approximately 20 g of the soil sample was heated at 80 °C for 48 h to estimate the water content from the weight loss and water-filled pore space (WFPS; the calculation was detailed in Text S1). Using the remaining soil sample (120 g), NH_4^+, NO_3^-, and NO_2^- in each soil sample were extracted into 120 mL of a 2-M KCl solution, and their concentrations were determined using a high performance microflow analyzer (QuAAtro 39 Autoanalyzer, BLTEC, Osaka, Japan).

删除了: an autoanalyzer

2.4 Concentration and isotopic compositions of N_2O

The gas samples collected in aluminum bags or stainless canisters were subsampled into a 100-ml pre-evacuated glass bottle to determine the concentration ([N_2O]), $\delta^{15}N$, and $\delta^{18}O$ of N_2O simultaneously. The remaining samples were further subsampled to either 1 or 2 L pre-evacuated glass bottles to determine the $\Delta^{17}O$ of N_2O. The concentration and isotopic compositions ($\delta^{15}N$, $\delta^{18}O$, and $\Delta^{17}O$) of N_2O were determined using a continuous flow isotope ratio mass spectrometry (CF-IRMS; Finnigan MAT252, Thermo Fisher Scientific, Waltham, MA, USA) system that consists of an original pre-concentrator system, chemical traps, and gas chromatograph at Nagoya University (Komatsu et al., 2008). The analytical procedures using the CF-IRMS system were the same as those detailed in previous studies (Hirota et al., 2010; Komatsu et al., 2008).

The isotopic ratios of $^{15}N/^{14}N$, $^{17}O/^{16}O$, and $^{18}O/^{16}O$ are expressed in the δ notations:

$$\delta^{15}N,\ \delta^{17}O,\ \text{or}\ \delta^{18}O = R_{sample}/R_{standard} - 1 \quad (1)$$

where R denotes $^{15}N/^{14}N$, $^{17}O/^{16}O$, or $^{18}O/^{16}O$ ratios of the sample and each standard reference material.

The $\Delta^{17}O$ of N_2O, including NO_2^-, NO_3^-, H_2O, and O_2, is defined by Eq. 2 (Kaiser et al., 2007; Miller, 2002):

$$\Delta^{17}O = \frac{1+\delta^{17}O}{(1+\delta^{18}O)^{\beta}} - 1 \quad (2)$$

where β denotes the slope of the reference line in the $\delta^{17}O$–$\delta^{18}O$ space. Previous studies have proposed values ranging from 0.525 to 0.5305 for β during the various processes of isotope fractionation through experimental measurements and/or theoretical calculations (Cao and Liu, 2011; Matsuhisa et al., 1978; Pack and Herwartz, 2014; Sharp and Wostbrock, 2021). In this study, we adopted a value of 0.528 for β to define $\Delta^{17}O$. The details of the ranges of the possible $\Delta^{17}O$ variations due to the ranges of β are presented in Section 4.1.

To calibrate the $\delta^{15}N$ and $\delta^{18}O$ of N_2O to the international scale, N_2O in a tropospheric air sample collected at Hateruma Island in 2010 (Japan) was used as the standard with a $\delta^{15}N$ value of +6.5 ‰ and a $\delta^{18}O$ value of +44.3 ‰ (Toyoda et al., 2013). To calibrate the $\Delta^{17}O$ of N_2O on the international VSMOW (Vienna Standard Mean Ocean Water) scale, we prepared two kinds of N_2O standards with different $\Delta^{17}O$ values calibrated using a conventional method (Thiemens and Trogler, 1991). The procedures for this calibration are presented in Section 2.6, with the details of the N_2O standards. Through repeated measurements of N_2O in a tropospheric air sample collected at Nagoya University, the analytical precisions (1σ) of the measurements were estimated to be ±10.0 ppb, ±0.5 ‰, ±0.6 ‰, and ±0.11 ‰ for concentration, $\delta^{15}N$, $\delta^{18}O$, and $\Delta^{17}O$, respectively (Figure S2). To achieve higher precision, analyses of $\Delta^{17}O$ were performed at least three times for each sample, resulting in a standard error (SE) of ±0.06 ‰.

2.5 Emission flux

Based on the change in the concentration of N_2O from the inlet to the outlet, the emission flux of N_2O from the soil was calculated using Eq. 3:

$$\text{Flux} = \frac{P \times V \times (C_{final} - C_{air}) \times M}{R \times T \times t \times A} \quad (3)$$

where Flux denotes the emission flux of N_2O (μg N m^{-2} h^{-1}), P denotes the pressure (Pa), V represents the volume of the gas sample in the aluminum bag (0.0045 m^3), C_{final} denotes the concentration of N_2O in the gas sample taken at the end of each deployment of the chamber (μmol mol^{-1}), C_{air} denotes the concentration of N_2O in the ambient air (μmol mol^{-1}), M represents the molecular weight of N in N_2O (28 μg N μmol^{-1}), R represents the universal gas constant (8.314 m^3 Pa K^{-1} mol^{-1}), T represents the air temperature in the forest (K), t represents the duration of each gas sampling (45 min), and A represents the surface area of soil covered by the chamber (0.24 m^2).

2.6 Calibration of the $\Delta^{17}O$ values of N_2O

To determine the $\Delta^{17}O$ values of N_2O in the samples on the VSMOW scale, we prepared two standards (STD1 and STD2) containing N_2O. The $\Delta^{17}O$ values of N_2O in the standards were calibrated to the VSMOW scale using the conventional method reported in (Thiemens and Trogler, 1991), where N_2O was quantitatively converted to O_2 using BrF_5 and a Ni catalytic container. The details are presented below.

A calibrated quantity of N_2O (50–170 μmol) was subsampled and transferred into a nickel tube (approximately 60 cm^3) under liquid N_2 temperature. The coexisting components of N_2O, such as helium in the case of STD2, were evacuated from the nickel tube after N_2O was trapped in the nickel tube under liquid N_2 temperature. The nickel

tube was then heated at 725 °C for 2.5 h to convert N_2O to NiO and N_2. After evacuating N_2 from the nickel tube, a 10-fold quantity of BrF_5 was introduced into the nickel tube and heated at 725 °C for 12 h to convert NiO to O_2 and NiF_2. After the purification of O_2, both $\delta^{18}O$ and $\Delta^{17}O$ of O_2 were determined on the VSMOW scale using IRMS, with the quantity of O_2 evolved from N_2O. Details on the procedures of O_2 purification and the measurement of O_2 using IRMS on the VSMOW scale have been described in previous studies (Sambuichi et al., 2021, 2023). STD1 is pure N_2O gas prepared from N_2O in a gas cylinder (more than 99.9 %; Koike Medical Ltd., Japan). The yield ratio of O_2 and $\Delta^{17}O$ of STD1 were 103±7 % and −0.22±0.07 ‰, respectively (Figure S3). The N_2O in STD2 is a mixture of helium and N_2O (N_2O/He ≈ 1.5) produced from NO_2^- that had been under oxygen isotope exchange equilibrium with H_2O with a $\Delta^{17}O$ value of +1.2 ‰ originally, under a pH of 1.2. NO_2^- was then converted to N_2O through a reaction with hydrazoic acid (N_3H), as described by (Tsunogai et al., 2008). The reaction product (N_2O) was purged from the vial using pure helium (more than 99.9 %). After the removal of H_2O by passing a trap under the temperature of dry ice + ethanol, N_2O was captured in a trap at the temperature of liquid O_2 and then transported into a 1-L stainless steel canister together with helium. The yield of O_2 and $\Delta^{17}O$ of STD2 were 97±5 % and +1.13±0.02 ‰, respectively (Figure S3). To calibrate the $\Delta^{17}O$ values of the samples measured using CF-IRMS, approximately 1 mL of each STD was subsampled into a 200-mL pre-evacuated glass bottle and diluted using pure helium to 1 atm. The $\Delta^{17}O$ values of N_2O in the diluted standards were then determined using CF-IRMS like the procedure used on the samples before the sample measurements by introducing 30–60 nmol of N_2O.

This allowed us to calibrate the $\Delta^{17}O$ values of the samples to the VSMOW scale (Figure S4).

2.7 Isotopic composition of NO_2^-

To determine the $\delta^{18}O$ and $\Delta^{17}O$ values of soil NO_2^- that had been extracted in the KCl solution, the NO_2^- in the KCl solution was chemically converted to N_2O using the method originally developed to determine the $\delta^{18}O$ of NO_2^- (McIlvin and Altabet, 2005), with several modifications for $\Delta^{17}O$ (Xu et al., 2021), as explained below. Approximately 40 mL of each solution was pipetted into a glass vial (66.7 mL) and sealed with a butyl rubber septum cap. After purging the solution using high-purity helium for 45 min, 1.8 mL of an azide-acetic acid buffer (0.1 mol L^{-1} NaN_3 in 1 vol. % acetic acid), which had been purged using pure helium as well, was added to the solution to convert NO_2^- to N_2O:

$$HNO_2 + HN_3 \rightarrow N_2O + H_2O + N_2 \quad \text{(R1)}$$

After the vials were shaken for 1 h at a rate of 2 cycles s^{-1}, 0.9 mL of 6-M NaOH was added to each vial and shaken for 15 min.

The $\delta^{18}O$ and $\Delta^{17}O$ of N_2O converted from NO_2^- in each vial were determined using the CF-IRMS system. We repeated the analyses for each solution sample at least three times to obtain better precision for $\Delta^{17}O$.

The $\delta^{18}O$ values of NO_2^- were calibrated to the VSMOW scale using three in-house nitrite standards (STD10, STD11, and STD12), the $\delta^{18}O$ values of which had been determined using a thermal conversion/elemental analyzer IRMS system, where oxygen atoms in each nitrite/nitrate had been converted into CO using a glassy carbon tube at

1400 °C (Xu et al., 2021) and calibrated to the VSMOW scale using the international nitrate standards USGS34 ($\delta^{18}O$ = −27.9 ‰) and IAEA-NO-3 ($\delta^{18}O$ = +25.6 ‰) as the primary standards. Isotope fractionations during chemical conversion into N_2O were corrected by measuring the nitrite standards in the same way as samples were measured using the CF-IRMS system. In addition, the extent of oxygen isotope exchange between NO_2^- and H_2O during the conversion was quantified using the relation between $\delta^{18}O$ of the nitrite standards and that of N_2O (Xu et al., 2021). The $\Delta^{17}O$ values of NO_2^- were calibrated to the VSMOW scale by comparing N_2O derived from NO_2^- with N_2O standards (STD1 and STD2) while assuming that the changes in $\Delta^{17}O$ were negligible during the conversion from NO_2^- into N_2O, except for the oxygen isotope exchange reaction between NO_2^- and H_2O during the conversion to N_2O. The progress of oxygen isotope exchange between NO_2^- and H_2O was calibrated from the $\Delta^{17}O$ values of NO_2^- using the exchange rate estimated by calculating $\delta^{18}O$ values while assuming that the $\Delta^{17}O$ value of H_2O was 0 ‰.

While the KCl solutions were widely used for the extraction of soil NO_2^- (e.g., Lewicka-Szczebak et al., 2021; Shen et al., 2003), Homyak et al. (2015) raised the concerns that the recovery of soil NO_2^- could be low when using KCl solutions compared to deionized water. Therefore, we conducted a comparative experiment to evaluate this potential issue and concluded that the use of KCl solution introduced negligible bias in terms of soil NO_2^- recovery or $\Delta^{17}O$ measurements compared to deionized water extraction for the soil type and experimental conditions in this study. The details are described in the supplement (Text S2).

3. Results

3.1 Flux and isotopic compositions of N_2O emitted from forested soil

Almost all of the concentrations of N_2O ([N_2O]) in the samples collected in aluminum bags were higher than that of N_2O in ambient air (Figures 3a and S5), implying that N_2O in the aluminum bags was a mixture of N_2O in ambient air and N_2O emitted from the forested soil. To determine the isotopic compositions ($\delta^{15}N$, $\delta^{18}O$, and $\Delta^{17}O$) of N_2O emitted from the soil, N_2O derived from ambient air was excluded using the linear correlation between 1/[N_2O] and the isotopic compositions ($\delta^{15}N$, $\delta^{18}O$, and $\Delta^{17}O$) during mixing (Figures 3b, 3c, 3d, and S5), also was known as Keeling plot approach (Keeling, 1958; Tsunogai et al., 1998, 2003). This method assumes that the concentrations of N_2O ($N_2O/(N_2O + N_2)$) in the gases emitted from the soil were more than 3 %, allowing 1/[N_2O] to be approximated to be 0 (Text S3). The uncertainties associated with the isotopic compositions of N_2O emitted from soil (i.e., the intercept) were estimated by applying the York method (Tsunogai et al., 2011; York et al., 2004) to the obtained relationship between 1/[N_2O] as the independent variable and the isotopic compositions as the dependent variable in which uncertainties of both independent and dependent variables for individual data are considered.

The flux of N_2O emitted from the forested soil determined on fine days varied from −0.2 to 9.8 μg N m^{-2} h^{-1}, with an average of 3.8±3.1 μg N m^{-2} h^{-1} (1SD; n = 12). In addition, the emission flux during the warm seasons (from April to October; 5.1±2.8 μg N m^{-2} h^{-1}) was significantly higher than that during the cold seasons (from November to March; 1.0±1.1 μg N m^{-2} h^{-1}) (Figure 4a; Table S1), implying that the emission flux of

删除了: 2

317 N_2O on fine days exhibited clear seasonal variation. Furthermore, the average emission
318 flux of N_2O determined on rainy days (38.8±28.0 μg N m^{-2} h^{-1}; n = 6) was significantly
319 higher than that determined on fine days (3.8±3.1 μg N m^{-2} h^{-1}) (Figures 4a and 4b).
320 These patterns of N_2O emissions were in accordance with those of agricultural and
321 forested soils reported in previous studies (Anthony et al., 2023; Chen et al., 2012;
322 Choudhary et al., 2002; Yan et al., 2008).
323 Because of the small emission flux of N_2O during the cold seasons, the linear
324 relationships between the isotopic compositions and 1/[N_2O] became insignificant in
325 some of the observations performed during the cold seasons (Figure S5, from Nov. 2022
326 to Jan. 2023). Thus, the uncertainties associated with the isotopic compositions estimated
327 for N_2O emitted from the soil became enormous. Consequently, the isotopic
328 compositions of N_2O emitted from the soil are not shown under the following conditions:
329 (1) the [N_2O] in the gas sample collected at the end of each deployment of the chamber
330 did not exceed 130 % of that of ambient air, and (2) the linear correlation between
331 1/[N_2O] and the isotopic compositions was statistically insignificant ($P > 0.05$). Similar
332 criteria have been adopted in previous studies (Kaushal et al., 2022; Opdyke et al., 2009).
333 The N_2O emitted from the forested soil on fine days exhibited $\delta^{15}N$, $\delta^{18}O$, and $\Delta^{17}O$
334 values ranging from −27.5 ‰ to −17.9 ‰, from +26.1 ‰ to +37.6 ‰, and from −0.40 ‰
335 to −0.11 ‰, respectively, with average values and standard deviations (1SD) of
336 −22.5±2.8 ‰, +30.9±4.3 ‰, and −0.30±0.09 ‰, respectively (Figures 4g, 4e, and 4c).
337 On the other hand, N_2O emitted from the forested soil on rainy days exhibited $\delta^{15}N$, $\delta^{18}O$,
338 and $\Delta^{17}O$ values ranging from −26.6 ‰ to −13.8 ‰, from +18.4 ‰ to +36.2 ‰, and from

−0.06 ‰ to +0.26 ‰, respectively, with average values and standard deviations (1SD) of −20.4±5.0 ‰, +27.9±6.4 ‰, and +0.12±0.13 ‰, respectively (Figures 4g, 4e, and 4c).

The NO_2^- exhibited $\delta^{18}O$ and $\Delta^{17}O$ values ranging from +2.4 ‰ to +12.0 ‰ and from +0.04 to +0.50 ‰, respectively, with average values of +6.0±2.0 ‰ and +0.23±0.12 ‰, respectively (n = 18, Figures 4e and 4c). These $\delta^{18}O$ values of NO_2^- coincided well with those determined in a previous study (Lewicka-Szczebak et al., 2021).

3.2 Flux and isotopic compositions of N_2O emitted from artificially fertilized soils

The fluxes of N_2O emitted from the NF (no fertilizer), U (fertilized with urea, $CO(NH_2)_2$), and CS (fertilized with Chile saltpeter, KNO_3) plots were 5.2, 70.6, and 112.3 μg N m^{-2} h^{-1}, respectively, 2 days after fertilization and 4.2, 56.7, and 39.4 μg N m^{-2} h^{-1}, respectively, 6 days after fertilization (Table S1). The fluxes of N_2O emitted from the U and CS plots were significantly higher than that from the NF plot, indicating that the flux of N_2O emitted from the soil increased significantly because of fertilization, supporting the results reported in previous studies (Kaushal et al., 2022; McKenney et al., 1978; Toyoda et al., 2011, 2017).

The $\delta^{15}N$, $\delta^{18}O$, and $\Delta^{17}O$ values of N_2O emitted from the NF plot 2 days after fertilization were −17.1±6.4 ‰, +36.1±6.7 ‰, and −0.37±0.20 ‰, respectively, whereas those emitted from the NF plot 6 days after fertilization were −12.2±3.2 ‰, +40.0±13.3 ‰, and −0.32±0.23 ‰, respectively. The $\delta^{15}N$, $\delta^{18}O$, and $\Delta^{17}O$ values of N_2O emitted from the U plot 2 days after fertilization were −39.3±0.7 ‰, +34.4±0.4 ‰, and −0.14±0.06 ‰, respectively, whereas those emitted from the U plot 6 days after fertilization were −33.3±0.5 ‰, +25.7±0.6 ‰, and −0.16±0.05 ‰, respectively. The

362 $\delta^{15}N$, $\delta^{18}O$, and $\Delta^{17}O$ values of N_2O emitted from the CS plot 2 days after fertilization
363 were −19.3±0.6 ‰, +54.1±0.8 ‰, and +8.22±0.03 ‰, respectively, whereas those
364 emitted from the CS plot 6 days after fertilization were −11.3±0.7 ‰, +58.7±1.2 ‰, and
365 +7.36±0.17 ‰, respectively (Figure 5). These flux, $\delta^{15}N$, and $\delta^{18}O$ of N_2O emitted from
366 the NF, U, and CS plots correspond well with the results of many previous studies on
367 forested and artificial soils (or agricultural soils) (Kaushal et al., 2022; Kim and Craig,
368 1993; Snider et al., 2009; Toyoda et al., 2017; Wrage et al., 2004).
369 The $\delta^{18}O$ and $\Delta^{17}O$ values of NO_2^- in the NF plot 2 days after fertilization were
370 +2.7 ‰ and +0.42 ‰, respectively, whereas those in the NF plot 6 days after fertilization
371 were +1.3 ‰ and +0.35 ‰, respectively. The $\delta^{18}O$ and $\Delta^{17}O$ values of NO_2^- in the U plot
372 2 days after fertilization were +7.6 ‰ and +0.31 ‰, respectively, whereas those in the U
373 plot 6 days after fertilization were +5.4 ‰ and +0.17 ‰, respectively. The $\delta^{18}O$ and $\Delta^{17}O$
374 values of NO_2^- in the CS plot 2 days after fertilization were +29.0 ‰ and +8.26 ‰,
375 respectively, whereas those in the CS plot 6 days after fertilization were +45.2 ‰ and
376 +12.32 ‰, respectively (Figure 6).
377

378 **4. Discussion**

379 **4.1 Identification of N_2O production pathways in forested soil using $\Delta^{17}O$ signature**

380 Because O atoms in N_2O emitted from soil can be derived from those in NO_2^-, O_2, or
381 H_2O in soil (Figure 1), we can constrain the pathways of N_2O production by comparing
382 the $\delta^{18}O$ and $\Delta^{17}O$ values of N_2O with those of NO_2^-, O_2, and H_2O in soil. Consequently,
383 we compiled the $\delta^{18}O$ and $\Delta^{17}O$ values of atmospheric O_2 (+23.88 ‰ for $\delta^{18}O$ and
384 −0.44 ‰ for $\Delta^{17}O$, (Sharp and Wostbrock, 2021)) and rainwater (ranging from −2 ‰ to

删除了: of
删除了: pathways
删除了: tropospheric
删除了:
删除了: H_2O
删除了: (

391 −10 ‰ for $\delta^{18}O$ in Japan, (Nakagawa et al., 2018; Takahashi, 1998; Uechi and Uemura,
392 2019; Zou et al., 2015); +0.03 ‰ for $\Delta^{17}O$ in Japan (Uechi and Uemura, 2019)), as
393 shown in Figures 4 and 6, along with those of soil NO_2^- measured in this study.
394 The $\Delta^{17}O$ of N_2O produced in the soil may differ from that of the source of O atoms
395 (O_2, NO_2^-, H_2O) because of oxygen isotope fractionation during nitrification and
396 denitrification, as the value of β in Eq. (2) may vary depending on the reactions. Thus,
397 prior to using $\Delta^{17}O$ values to identify the pathways of N_2O production in soils, we
398 quantified the possible variations in the $\Delta^{17}O$ values of N_2O during each reaction. The
399 details are presented below.
400 The fractionation of oxygen isotopes during the transformation of the O atoms in O_2 to
401 those in N_2O through nitrification accompanies significant variations in the value of $\delta^{18}O$
402 from O_2 to N_2O (Figures 4e and 6a). In addition to $\delta^{18}O$, the $\Delta^{17}O$ value of N_2O produced
403 through nitrification could be somewhat different from that of O_2, even if all O atoms in
404 N_2O were derived from O_2, due to the possible differences in β from 0.528 during the
405 reaction (Figure 7). The average variation in $\delta^{18}O$ from O_2 to N_2O due to nitrification
406 ($\Delta\delta^{18}O$ (N_2O-O_2)) was estimated to be 9 ‰ on average (Figures 4e and 6a) based on the
407 difference in $\delta^{18}O$ values between N_2O emitted from the soil in this study (+33±10 ‰; n
408 = 19) and O_2 in the literature (Sharp and Wostbrock, 2021). Conversely, we can expect
409 values from 0.525 to 0.5305 for β in the various reactions (Cao and Liu, 2011; Matsuhisa
410 et al., 1978; Pack and Herwartz, 2014; Sharp and Wostbrock, 2021), where the β of
411 nitrification may be included. Thus, we quantified the possible range of variations in the
412 $\Delta^{17}O$ value of N_2O from that of O_2 to be less than 0.027 ‰ (Figure 7), based on the
413 observed $\Delta\delta^{18}O(N_2O-O_2)$ and the possible variation range of β.

删除了: ,

删除了: ↵

Similarly, the fractionation of oxygen isotopes during the transformation of O atoms in NO_2^- to those in N_2O through denitrification accompanies significant variations in $\delta^{18}O$ from NO_2^- to N_2O as well. The $\Delta^{17}O$ value of N_2O produced through NO_2^- reduction could be somewhat different from that of NO_2^-, even if all O atoms in N_2O were derived from NO_2^-, due to the possible differences in β from 0.528 during the reaction (Figure 7). The average variation in $\delta^{18}O$ from NO_2^- to N_2O due to fractionation ($\Delta\delta^{18}O$ ($N_2O-NO_2^-$)) was estimated to be 25 ‰ on average (Figures 4e and 6a) based on the difference in $\delta^{18}O$ values between N_2O (+33±10 ‰; n = 19) and NO_2^- in this study (+8±9 ‰; n = 24). Thus, we quantified the possible range of variations in the $\Delta^{17}O$ value of N_2O from that of NO_2^- to be less than 0.075 ‰ (Figure 7), based on the observed $\Delta\delta^{18}O$ ($N_2O-NO_2^-$) and the possible variation range of β, from 0.525 to 0.5305.

Similarly, kinetic fractionation during the reduction of N_2O to N_2 accompanies variation in $\delta^{18}O$ from original N_2O to residual N_2O as well. The $\Delta^{17}O$ value of residual N_2O could somewhat differ from that of the original N_2O. Previous studies have reported the range of variations in $\delta^{18}O$ from original N_2O to residual N_2O due to kinetic fractionation to be less than 10 ‰ on average through incubation experiments (Lewicka-Szczebak et al., 2014, 2015). Thus, we quantified the possible range of variations in the $\Delta^{17}O$ value of residual N_2O from that of original N_2O to be less than 0.03 ‰ (Figure 7), based on $\Delta\delta^{18}O$ (less than 10 ‰) and the variation range of β, from 0.525 to 0.5305.

These possible variations in $\Delta^{17}O$ (less than 0.075 ‰) were much less than the difference in $\Delta^{17}O$ values between O_2 and NO_2^- in the forested soil (0.7 ‰ on average; Figures 4c). In addition, the possible variation ranges in $\Delta^{17}O$ become much smaller if the differences in β from 0.528 were smaller than those used in the calculations (from 0.525

to 0.5305). Thus, we concluded that the possible variations in the $\Delta^{17}O$ value of N_2O from that of the source molecules of O atoms (O_2, H_2O, and NO_2^-) during the transformations, including nitrification, denitrification, and reduction, were negligible.

While the $\Delta^{17}O$ values of soil O_2 and H_2O used in this study were referred from atmospheric O_2 and rainwater, respectively, the processes in soil, including diffusion and respiration of O_2 and evaporation and infiltration of rainwater, may cause significant isotopic fractionations of $\delta^{18}O$, which could consequently alter the $\Delta^{17}O$ values of atmospheric O_2 and rainwater. Thus, prior to using $\Delta^{17}O$ values to identify the pathways of N_2O production in soils, we evaluated the possible variations in the $\Delta^{17}O$ values of O_2 and H_2O in soil compared to those of atmospheric O_2 and rainwater. The details are presented below.

For soil O_2, Aggarwal and Dillon (1998) measured the $\delta^{18}O$ values in soil gas at a depth of 3-4 m at a site near Lincoln, Nebraska, USA ranged from +23.3 ‰ to +27.2 ‰, showing the values were comparable with that of atmospheric O_2 (+23.5 ‰ after adjustment in Aggarwal and Dillon. 1998). This confirms that the isotopic fractionations of soil O_2 induced from soil respiration and diffusion processes weren't significant. Because the maximum variation in $\delta^{18}O$ from atmospheric O_2 to soil O_2 was less than 3.7 ‰ (27.2 ‰ − 23.5 ‰), using the method presented in Figure 7, we quantified the possible variations in the $\Delta^{17}O$ value of soil O_2 from that of atmospheric O_2 to be less than 0.01 ‰. Thus, we ignored the negligible variations in this study.

Similarly, for soil H_2O, Lyu (2021) observed that $\delta^{18}O$ values in soil H_2O at the depths of 0-5 cm, 15-20 cm, and 40-45 cm in a subtropical forest plantation ranged from −4 ‰ to −10 ‰, which fully overlapped with local rainwater (−1 ‰ to −16 ‰), indicating

insignificant isotopic fractionations of soil H_2O during hydrological processes such as infiltration and evaporation. Besides, Aron et al. (2021) compiled $\Delta^{17}O$ values of terrestrial H_2O including rainwater, surface and subsurface water in earth, ranged from +0.06 to −0.06 ‰ and didn't show significant difference with each other, which also indicating that the possible variations of $\Delta^{17}O$ values of soil H_2O compared to that of rainwater should be negligible. Finally, we added the variations of $\Delta^{17}O$ values (+0.06 to −0.06 ‰) of terrestrial H_2O reported in Aron et al. (2021) to Figures 4 and 6 as the uncertainties of $\Delta^{17}O$ values of soil H_2O.

In the forested soil, N_2O exhibited $\Delta^{17}O$ values (−0.30±0.09 ‰ on average) that were close to that of O_2 (−0.44 ‰) but deviated from those of soil NO_2^- on fine days (+0.24±0.14 ‰; Figures 4c and 4d), implying that nitrification was the main pathway to produce N_2O in the soil on fine days. Conversely, N_2O emitted from the soil on rainy days exhibited $\Delta^{17}O$ values (+0.12±0.13 ‰) that were close to those of soil NO_2^- (+0.22±0.09 ‰) and soil H_2O (+0.03 ‰) but deviated from that of O_2 (Figures 4c and 4d), implying that (1) the main pathway to produce N_2O changed from nitrification on fine days to denitrification on rainy days and/or (2) the possible contribution of O atoms derived from soil H_2O became more active during the production of N_2O in the soil on rainy days.

4.2 Changes in the $\Delta^{17}O$ of N_2O emitted from artificially fertilized soils

To quantitatively constrain the possible contributions of O atoms derived from soil H_2O during the production of N_2O in the soil, we observed changes in the isotopic compositions of N_2O from the same soil in response to artificial fertilization. In the plot

fertilized with CS, the $\Delta^{17}O$ value of N_2O emitted from the soil (+7.79±0.61 ‰ on the average of 2 and 6 days after the fertilization) became significantly closer to that of soil NO_2^- (+10.3±2.9 ‰) compared with that of atmospheric O_2 (−0.44 ‰; Figure 6b). This suggested that denitrification became the main pathway of N_2O production, probably because of fertilization, which resulted in a significantly higher concentration of NO_3^- (278.4±43.2 mg N kg^{-1}; Table S1) than that of NH_4^+ (15.8±4.1 mg N kg^{-1}) in the CS plot. In addition, N_2O emitted from the CS plot exhibited $\Delta^{17}O$ values that were significantly different from those of soil H_2O (+0.03 ‰; Figure 6b), implying that the contribution of O atoms derived from soil H_2O was minor during the reduction of NO_2^- to produce N_2O. If all the O atoms with low $\Delta^{17}O$ values in N_2O were derived from soil H_2O (+0.03 ‰) in the CS plot, the contribution of O atoms derived from soil H_2O was calculated to be 24 % ((10.30 ‰ – 7.79 ‰) / (10.30 ‰ – 0.03 ‰)), based on the isotopic mass balance. If the O_2 also contributed to the N_2O production in the CS plot, the contribution of O atoms derived from soil H_2O should be further reduced. As a result, we determined that the maximum possible contribution of O atoms derived from soil H_2O during the reduction of NO_2^- to N_2O was 24 %.

删除了: The maximum possible contribution of O atoms derived from soil H_2O during the reduction of NO_2^- to N_2O was 24 %.

On the other hand, in the plot fertilized with urea (U plot), the $\Delta^{17}O$ value of N_2O (−0.15±0.01 ‰) was close to that of O_2 (−0.44 ‰) compared with that of soil NO_2^- (+0.24±0.10 ‰). This suggested that nitrification was the main pathway of N_2O production (Figure 6b), probably due to the enhancement of NH_4^+ concentration (423.1±18.2 mg N kg^{-1}; Table S1) compared with that of NO_3^- (13.0±10.7 mg N kg^{-1}) in the U plot. In addition, N_2O emitted from the U plot exhibited $\Delta^{17}O$ values that were significantly different from that of soil H_2O (+0.03 ‰; Figure 6b), implying that the

511 contribution of O atoms derived from soil H_2O was also minor during the oxidation of
512 NH_4^+ to produce N_2O. Consequently, the contribution of O atoms derived from soil H_2O
513 was minor in the soil during N_2O production, irrespective of the pathways of N_2O
514 production being either nitrification or denitrification. In addition, it is difficult to explain
515 the observed increases in the emission flux of N_2O from the soil on rainy days based only
516 on the active contribution of O atoms derived from soil H_2O. Consequently, we
517 concluded that N_2O production through denitrification became active in the soil on rainy
518 days, which resulted in increased N_2O emission and higher $\Delta^{17}O$ values.
519
520 **4.3 Verification of active N_2O emission by denitrification on rainy days**
521 The forested soil exhibited significantly lower WFPS on fine days (66.1±6.2 %; Table
522 S1) than on rainy days (95.6±19.1 %), implying that the O_2 concentration in the soil was
523 higher on fine days than on rainy days. Using the isotope tracer enriched in ^{15}N ($^{15}NO_3^-$
524 or $^{15}NH_4^+$), Mathieu et al. 2006 estimated the relative importance of nitrification and
525 denitrification to produce N_2O in soil. They found that nitrification produced the majority
526 of N_2O under low WFPS conditions (75 %), whereas denitrification accounted for more
527 than 85 % of N_2O produced under high WFPS conditions (150 %). Similarly, using
528 natural stable isotopes (SP), Ibraim et al. 2019 reported the primary pathway for N_2O
529 production in a grassland shifted from nitrification to denitrification as increasing WFPS,
530 when WFPS was below 90 %. Thus, we conclude that the lower WFPS in the soil caused
531 oxic conditions on fine days, resulting in nitrification as the primary pathway for N_2O
532 production in the soil. Conversely, the higher WFPS caused redox conditions in the soil

on rainy days, resulting in active N_2O production through denitrification in the soil (Figures 4a and 4b).

During continuous monitoring of the emission flux of N_2O from an agricultural soil for four years, Anthony et al. 2023 found short-term increases in the emission flux during or immediately after rainfall or irrigation. They referred to this high emission flux as "hot moments" and defined it as exceeding four standard deviations of that of normal periods. They also found significant correlations between the emission flux and WFPS, leading to the conclusion that variations in the concentrations of O_2 in surface soils were responsible for the hot moments of N_2O emissions. Although the hot moments accounted for 1 % of all measurements, they contributed up to 57 % of the annual emissions, indicating their significance as a source of atmospheric emissions. In this study, the emission flux of N_2O on rainy days also exceeded four standard deviations of that on fine days (Figures 4a and 4b). The $\Delta^{17}O$ evidence of N_2O found in this study further verified that denitrification was mainly responsible for the enhancement of N_2O production during the hot moments.

4.4 Changes in the pathway of N_2O production due to fertilization with urea

During our observation on the plot fertilized with urea (U plot), N_2O emitted from the plot exhibited $\Delta^{17}O$ values (−0.15±0.01 ‰ on average; Figure 6b) that were significantly higher than those of the plot without fertilization (NF plot; −0.35±0.04 ‰ on average). Although an increase in the contribution of O atoms derived from soil H_2O could be responsible for the $\Delta^{17}O$ values in addition to an increase in N_2O production through nitrification, we concluded that an increase in N_2O production through NO_2^- reduction

555 was responsible for the $\Delta^{17}O$ values (−0.15±0.01 ‰ on average) of N_2O produced in the
556 plot in response to fertilization of urea/NH_4^+ for the following reasons.
557 Avrahami et al. 2002 reported that fertilization with urea/NH_4^+ in soil promoted the
558 oxidation of NH_4^+ and thus provided electron acceptors for denitrification. That is, the
559 enrichment of nitrate through nitrification also promotes denitrification. Based on the
560 stable isotopes of N_2O ($\delta^{15}N$, $\delta^{18}O$, and SP), along with in vitro acetylene blockage
561 experiments on agricultural soils fertilized with NH_4^+, Zhang et al. 2016 reported that
562 while 50 %−70 % of N_2O was produced through nitrification, nitrifier denitrification
563 ($NH_4^+ \rightarrow NO_2^- \rightarrow N_2O$) and/or heterotrophic denitrification ($NH_4^+ \rightarrow NO_3^- \rightarrow$
564 $NO_2^- \rightarrow N_2O$) accounted for 30 %–50 % of N_2O production. Similar results have also
565 been reported in previous studies. Although N_2O production through nitrification was
566 simulated by fertilization with urea/NH_4^+ in various soils, denitrification also accounted
567 for a significant portion of N_2O production (Kaushal et al., 2022; Khalil et al., 2004; Zhu
568 et al., 2013). In addition to nitrifier/heterotrophic denitrification, N_2O produced through
569 the anammox process ($NH_4^+ + NO_2^- \rightarrow N_2O$, Okabe et al., 2011; Tang et al., 2011;
570 Tsushima et al., 2007) can be responsible for the reduction of NO_2^- as well. Zhu et al.
571 2011 found that the highest rate of anammox was comparable with that of denitrification
572 in soils fertilized with NH_4^+ (6.2−178.8 mg N kg^{-1}). These previous experiments support
573 our observation on the U plot that the addition of urea/NH_4^+ stimulates N_2O production
574 through nitrifier denitrification and/or heterotrophic denitrification, and/or anammox
575 reaction in addition to nitrification. The increased NO_3^- concentration in the U plot
576 (13.0±10.7 mg N kg^{-1}) compared with those in the NF plot (2.3±0.5 mg N kg^{-1}) probably

due to nitrification stimulated by the addition of NH_4^+ may be responsible for the active reduction of NO_2^-.

4.5 Stable $\Delta^{17}O$ as a natural signature for identifying N_2O production pathways

Although the $\delta^{18}O$ values of N_2O emitted from the soil were significantly higher than those of the sources of O atoms in N_2O (NO_2^-, O_2, and H_2O; Figures 4e and 6a) due to the fractionations of oxygen isotopes during the production and/or reduction of N_2O, the $\Delta^{17}O$ values of N_2O remained within the range of these sources. This indicates that $\Delta^{17}O$ primarily reflects the pathways of N_2O production, providing information distinct from the $\delta^{18}O$ signature because $\Delta^{17}O$ is stable during the processes of biogeochemical isotope fractionation. Moreover, while N_2O emission from the forested soil did not show significant differences in $\delta^{15}N$ and $\delta^{18}O$ values between fine and rainy days due to the fractionations of nitrogen and oxygen isotopes (Figures 4f and 4h), the significant difference in the $\Delta^{17}O$ values of N_2O between fine and rainy days (Figure 4d) highlights $\Delta^{17}O$ to be a promising natural signature for identifying the pathways of N_2O production in soils.

In addition to natural soils, the stable $\Delta^{17}O$ signature is expected to be useful for identifying the pathways of N_2O production in various ecosystems, such as agricultural soils and aquatic environments, where the isotopic fractionations of nitrogen and oxygen isotopes involving biogeochemical processes are significant as well. However, in order to identify the pathways of N_2O production quantitatively, the uncertainties, including the β values of each reaction during N_2O production and the contributions of O atoms derived

带格式的：缩进：首行缩进： 2 字符

删除了:

删除了: In addition to natural soils,

from soil H_2O during N_2O production, should be quantified precisely in the future studies.

删除了: .

5. Conclusions

Temporal variations in $\Delta^{17}O$ of N_2O emitted from forested soil were determined to identify the main pathway of N_2O production. Both $\Delta^{17}O$ values and fluxes of N_2O were significantly higher on rainy days compared to fine days. Besides, the $\Delta^{17}O$ values of N_2O emitted on rainy and fine days were close to those of soil NO_2^- and O_2, respectively. Because NO_2^- and O_2 were the source of O-atoms in N_2O production through denitrification and nitrification, respectively, we concluded that while nitrification dominated N_2O production on fine days, denitrification became active on rainy days, resulting in the N_2O flux increasing. In addition, the $\Delta^{17}O$ of N_2O emitted from the same soil fertilized with either Chile saltpeter or urea exhibited values that were significantly different from those of soil H_2O, implying that the contributions of O atoms derived from soil H_2O during N_2O production were minor. Furthermore, while N_2O emitted from the forested soil did not show significant differences in $\delta^{15}N$ and $\delta^{18}O$ values between fine and rainy days, the significant difference in the $\Delta^{17}O$ values of N_2O highlights $\Delta^{17}O$ to be a promising natural signature for identifying the pathways of N_2O production in soils, because $\Delta^{17}O$ is almost stable during isotope fractionation processes such as N_2O production and reduction.

Data availability. All the primary data are presented in the Supplement.

Author contributions. WD, UT, and FN designed the study. WD, TH, WR, MI, HX, and YK performed the field observations. WD, UT, TS and FN determined the concentrations and isotopic compositions of the samples. WD, TS, FN, and UT performed data analysis.

Competing interests. The authors declare that they have no conflict of interest.

Acknowledgments.

We thank the anonymous referees for their valuable remarks on an earlier version of this paper. We are grateful to the members of the Biogeochemistry Group at Nagoya University for their valuable support throughout this study. This work was supported by a Grant-in-Aid for Scientific Research from the Ministry of Education, Culture, Sports, Science, and Technology of Japan under grant numbers 22H00561, 17H00780, 22K19846, the Grant-in-Aid for Japan Society for the Promotion of Science Fellows under grant number 23KJ1088, the Yanmar Environmental Sustainability Support Association, the River Fund of the River Foundation, Japan, the Reiwa Environmental Foundation, and the National Research Foundation of Korea Grant from the Korean Government (MSIT; the Ministry of Science and ICT, NRF-2021M1A5A1065425, KOPRI-PN24011).

Reference

Aggarwal, P. K. and Dillon, M. A.: Stable Isotope Composition of Molecular Oxygen in Soil Gas and Groundwater: A Potentially Robust Tracer for Diffusion and Oxygen Consumption Processes, Geochimica et Cosmochimica Acta, 62, 577–584, https://doi.org/10.1016/S0016-7037(97)00377-3, 1998.

设置了格式: 字体: 小四, (国际) Times New Roman

649 Anthony, T. L., Szutu, D. J., Verfaillie, J. G., Baldocchi, D. D., and Silver, W. L.:
650 Carbon-sink potential of continuous alfalfa agriculture lowered by short-term nitrous
651 oxide emission events, Nature Communications, 14, 1926,
652 https://doi.org/10.1038/s41467-023-37391-2, 2023.

653 Aron, P. G., Levin, N. E., Beverly, E. J., Huth, T. E., Passey, B. H., Pelletier, E. M.,
654 Poulsen, C. J., Winkelstern, I. Z., and Yarian, D. A.: Triple oxygen isotopes in the water
655 cycle, Chemical Geology, 565, 120026, https://doi.org/10.1016/j.chemgeo.2020.120026,
656 2021.

657 Avrahami, S., Conrad, R., and Braker, G.: Effect of Soil Ammonium Concentration on
658 N_2O Release and on the Community Structure of Ammonia Oxidizers and Denitrifiers,
659 Applied and Environmental Microbiology, 68, 5685–5692,
660 https://doi.org/10.1128/AEM.68.11.5685-5692.2002, 2002.

661 Balderston, W. L., Sherr, B., and Payne, W. J.: Blockage by acetylene of nitrous oxide
662 reduction in *Pseudomonas perfectomarinus*, Applied and Environmental Microbiology,
663 31, 504–508, https://doi.org/10.1128/aem.31.4.504-508.1976, 1976.

664 Bateman, E. J. and Baggs, E. M.: Contributions of nitrification and denitrification to N_2O
665 emissions from soils at different water-filled pore space, Biology and Fertility of Soils,
666 41, 379–388, https://doi.org/10.1007/s00374-005-0858-3, 2005.

667 Cao, X. and Liu, Y.: Equilibrium mass-dependent fractionation relationships for triple
668 oxygen isotopes, Geochimica et Cosmochimica Acta, 75, 7435–7445,
669 https://doi.org/10.1016/j.gca.2011.09.048, 2011.

670 Chen, G. C., Tam, N. F. Y., and Ye, Y.: Spatial and seasonal variations of atmospheric
671 N_2O and CO_2 fluxes from a subtropical mangrove swamp and their relationships with soil
672 characteristics, Soil Biology and Biochemistry, 48, 175–181,
673 https://doi.org/10.1016/j.soilbio.2012.01.029, 2012.

674 Choudhary, M. A., Akramkhanov, A., and Saggar, S.: Nitrous oxide emissions from a
675 New Zealand cropped soil: tillage effects, spatial and seasonal variability, Agriculture,
676 Ecosystems & Environment, 93, 33–43, https://doi.org/10.1016/S0167-8809(02)00005-1,
677 2002.

678 Cliff, S. S., Brenninkmeijer, C. A. M., and Thiemens, M. H.: First measurement of the
679 $^{18}O/^{16}O$ and $^{17}O/^{16}O$ ratios in stratospheric nitrous oxide: A mass-independent anomaly,

设置了格式：字体：（默认）Times New Roman，小四，字体颜色：黑色

带格式的：正文，段落间距段后：0 磅，不调整西文与中文之间的空格，不调整中文和数字之间的空格，到齐到网格

设置了格式：字体颜色：黑色

Journal of Geophysical Research: Atmospheres, 104, 16171–16175, https://doi.org/10.1029/1999JD900152, 1999.

Decock, C. and Six, J.: An assessment of N-cycling and sources of N^2O during a simulated rain event using natural abundance ^{15}N, Agriculture, Ecosystems & Environment, 165, 141–150, https://doi.org/10.1016/j.agee.2012.11.012, 2013.

Dickinson, R. E. and Cicerone, R. J.: Future global warming from atmospheric trace gases, Nature, 319, 109–115, https://doi.org/10.1038/319109a0, 1986.

Ding, W., Tsunogai, U., Nakagawa, F., Sambuichi, T., Sase, H., Morohashi, M., and Yotsuyanagi, H.: Tracing the source of nitrate in a forested stream showing elevated concentrations during storm events, Biogeosciences, 19, 3247–3261, https://doi.org/10.5194/bg-19-3247-2022, 2022.

Ding, W., Tsunogai, U., Nakagawa, F., Sambuichi, T., Chiwa, M., Kasahara, T., and Shinozuka, K.: Stable isotopic evidence for the excess leaching of unprocessed atmospheric nitrate from forested catchments under high nitrogen saturation, Biogeosciences, 20, 753–766, https://doi.org/10.5194/bg-20-753-2023, 2023.

Ding, W., Tsunogai, U., and Nakagawa, F.: Bias in calculating gross nitrification rates in forested catchments using the triple oxygen isotopic composition ($\Delta^{17}O$) of stream nitrate, Biogeosciences, 21, 4717–4722, https://doi.org/10.5194/bg-21-4717-2024, 2024.

Hattori, S., Nuñez Palma, Y., Itoh, Y., Kawasaki, M., Fujihara, Y., Takase, K., and Yoshida, N.: Isotopic evidence for seasonality of microbial internal nitrogen cycles in a temperate forested catchment with heavy snowfall, Science of The Total Environment, 690, 290–299, https://doi.org/10.1016/j.scitotenv.2019.06.507, 2019.

Hirota, A., Tsunogai, U., Komatsu, D. D., and Nakagawa, F.: Simultaneous determination of $\delta^{15}N$ and $\delta^{18}O$ of N_2O and $\delta^{13}C$ of CH_4 in nanomolar quantities from a single water sample, Rapid Communications in Mass Spectrometry, 24, 1085–1092, https://doi.org/10.1002/rcm.4483, 2010.

Hiyama, T., Kochi, K., Kobayashi, N., and Sirisampan, S.: Seasonal variation in stomatal conductance and physiological factors observed in a secondary warm-temperate forest, Ecological Research, 20, 333–346, https://doi.org/10.1007/s11284-005-0049-6, 2005.

Homyak, P. M., Vasquez, K. T., Sickman, J. O., Parker, D. R., and Schimel, J. P.: Improving Nitrite Analysis in Soils: Drawbacks of the Conventional 2 M KCl Extraction, Soil Science Society of America Journal, 79, 1237–1242, https://doi.org/10.2136/sssaj2015.02.0061n, 2015.

Ibraim, E., Wolf, B., Harris, E., Gasche, R., Wei, J., Yu, L., Kiese, R., Eggleston, S., Butterbach-Bahl, K., Zeeman, M., Tuzson, B., Emmenegger, L., Six, J., Henne, S., and Mohn, J.: Attribution of N_2O sources in a grassland soil with laser spectroscopy based

设置了格式：字体颜色：黑色

带格式的：定义网格后自动调整右缩进，不要在相同样式的段落间增加间距

isotopocule analysis, Biogeosciences, 16, 3247–3266, https://doi.org/10.5194/bg-16-3247-2019, 2019.

Kaiser, J., Röckmann, T., and Brenninkmeijer, C. A. M.: Complete and accurate mass spectrometric isotope analysis of tropospheric nitrous oxide, Journal of Geophysical Research: Atmospheres, 108, https://doi.org/10.1029/2003JD003613, 2003.

Kaiser, J., Hastings, M. G., Houlton, B. Z., Röckmann, T., and Sigman, D. M.: Triple Oxygen Isotope Analysis of Nitrate Using the Denitrifier Method and Thermal Decomposition of N_2O, Analytical Chemistry, 79, 599–607, https://doi.org/10.1021/ac061022s, 2007.

Kaushal, R., Hsueh, Y.-H., Chen, C.-L., Lan, Y.-P., Wu, P.-Y., Chen, Y.-C., and Liang, M.-C.: Isotopic assessment of soil N_2O emission from a sub-tropical agricultural soil under varying N-inputs, Science of The Total Environment, 827, 154311, https://doi.org/10.1016/j.scitotenv.2022.154311, 2022.

Keeling, C. D.: The concentration and isotopic abundances of atmospheric carbon dioxide in rural areas, Geochimica et Cosmochimica Acta, 13, 322–334, https://doi.org/10.1016/0016-7037(58)90033-4, 1958.

Khalil, K., Mary, B., and Renault, P.: Nitrous oxide production by nitrification and denitrification in soil aggregates as affected by O_2 concentration, Soil Biology and Biochemistry, 36, 687–699, https://doi.org/10.1016/j.soilbio.2004.01.004, 2004.

Kim, K.-R. and Craig, H.: Nitrogen-15 and Oxygen-18 Characteristics of Nitrous Oxide: A Global Perspective, Science, 262, 1855–1857, https://doi.org/10.1126/science.262.5141.1855, 1993.

Komatsu, D. D., Ishimura, T., Nakagawa, F., and Tsunogai, U.: Determination of the $^{15}N/^{14}N$, $^{17}O/^{16}O$, and $^{18}O/^{16}O$ ratios of nitrous oxide by using continuous-flow isotope-ratio mass spectrometry, Rapid Communications in Mass Spectrometry, 22, 1587–1596, https://doi.org/10.1002/rcm.3493, 2008.

Kool, D. M., Wrage, N., Oenema, O., Dolfing, J., and Van Groenigen, J. W.: Oxygen exchange between (de)nitrification intermediates and H_2O and its implications for source determination of NO and N_2O: a review, Rapid Communications in Mass Spectrometry, 21, 3569–3578, https://doi.org/10.1002/rcm.3249, 2007.

Kool, D. M., Dolfing, J., Wrage, N., and Van Groenigen, J. W.: Nitrifier denitrification as a distinct and significant source of nitrous oxide from soil, Soil Biology and Biochemistry, 43, 174–178, https://doi.org/10.1016/j.soilbio.2010.09.030, 2011.

Lewicka-Szczebak, D., Well, R., Köster, J. R., Fuß, R., Senbayram, M., Dittert, K., and Flessa, H.: Experimental determinations of isotopic fractionation factors associated with N_2O production and reduction during denitrification in soils, Geochimica et Cosmochimica Acta, 134, 55–73, https://doi.org/10.1016/j.gca.2014.03.010, 2014.

Lewicka-Szczebak, D., Well, R., Bol, R., Gregory, A. S., Matthews, G. P., Misselbrook, T., Whalley, W. R., and Cardenas, L. M.: Isotope fractionation factors controlling

isotopocule signatures of soil-emitted N_2O produced by denitrification processes of various rates, Rapid Communications in Mass Spectrometry, 29, 269–282, https://doi.org/10.1002/rcm.7102, 2015.

Lewicka-Szczebak, D., Jansen-Willems, A., Müller, C., Dyckmans, J., and Well, R.: Nitrite isotope characteristics and associated soil N transformations, Scientific Reports, 11, 5008, https://doi.org/10.1038/s41598-021-83786-w, 2021.

Lin, W., Ding, J., Li, Y., Zhang, W., Ahmad, R., Xu, C., Mao, L., Qiang, X., Zheng, Q., and Li, Q.: Partitioning of sources of N_2O from soil treated with different types of fertilizers by the acetylene inhibition method and stable isotope analysis, European Journal of Soil Science, 70, 1037–1048, https://doi.org/10.1111/ejss.12782, 2019.

Luo, J., Ledgard, S. F., and Lindsey, S. B.: Nitrous oxide emissions from application of urea on New Zealand pasture, New Zealand Journal of Agricultural Research, 50, 1–11, https://doi.org/10.1080/00288230709510277, 2007.

Lyu, S.: Variability of δ^2H and $\delta^{18}O$ in Soil Water and Its Linkage to Precipitation in an East Asian Monsoon Subtropical Forest Plantation, Water, 13, 2930, https://doi.org/10.3390/w13202930, 2021.

Mathieu, O., Hénault, C., Lévêque, J., Baujard, E., Milloux, M.-J., and Andreux, F.: Quantifying the contribution of nitrification and denitrification to the nitrous oxide flux using ^{15}N tracers, Environmental Pollution, 144, 933–940, https://doi.org/10.1016/j.envpol.2006.02.005, 2006.

Matsuhisa, Y., Goldsmith, J. R., and Clayton, R. N.: Mechanisms of hydrothermal crystallization of quartz at 250 °C and 15 kbar, Geochimica et Cosmochimica Acta, 42, 173–182, https://doi.org/10.1016/0016-7037(78)90130-8, 1978.

McIlvin, M. R. and Altabet, M. A.: Chemical Conversion of Nitrate and Nitrite to Nitrous Oxide for Nitrogen and Oxygen Isotopic Analysis in Freshwater and Seawater, Analytical Chemistry, 77, 5589–5595, https://doi.org/10.1021/ac050528s, 2005.

McKenney, D. J., Wade, D. L., and Findlay, W. I.: Rates of N_2O evolution from N-fertilized soil, Geophysical Research Letters, 5, 777–780, https://doi.org/10.1029/GL005i009p00777, 1978.

Michalski, G., Böhlke, J. K., and Thiemens, M.: Long term atmospheric deposition as the source of nitrate and other salts in the Atacama Desert, Chile: New evidence from mass-independent oxygen isotopic compositions, Geochimica et Cosmochimica Acta, 68, 4023–4038, https://doi.org/10.1016/j.gca.2004.04.009, 2004.

Miller, M. F.: Isotopic fractionation and the quantification of ^{17}O anomalies in the oxygen three-isotope system: an appraisal and geochemical significance, Geochimica et

设置了格式： 字体：（默认）Times New Roman，小四，字体颜色：黑色

带格式的： 正文，段落间距段后：0 磅，不调整西文与中文之间的空格，不调整中文和数字之间的空格，到齐到网格

设置了格式： 字体颜色：黑色

Cosmochimica Acta, 66, 1881–1889, https://doi.org/10.1016/S0016-7037(02)00832-3, 2002.

Mulvaney, R. L. and Kurtz, L. T.: A New Method for Determination of ^{15}N-Labeled Nitrous Oxide, Soil Science Soc of Amer J, 46, 1178–1184, https://doi.org/10.2136/sssaj1982.03615995004600060012x, 1982.

Nakagawa, F., Tsunogai, U., Obata, Y., Ando, K., Yamashita, N., Saito, T., Uchiyama, S., Morohashi, M., and Sase, H.: Export flux of unprocessed atmospheric nitrate from temperate forested catchments: a possible new index for nitrogen saturation, Biogeosciences, 15, 7025–7042, https://doi.org/10.5194/bg-15-7025-2018, 2018.

Okabe, S., Oshiki, M., Takahashi, Y., and Satoh, H.: N_2O emission from a partial nitrification–anammox process and identification of a key biological process of N_2O emission from anammox granules, Water Research, 45, 6461–6470, https://doi.org/10.1016/j.watres.2011.09.040, 2011.

Opdyke, M. R., Ostrom, N. E., and Ostrom, P. H.: Evidence for the predominance of denitrification as a source of N_2O in temperate agricultural soils based on isotopologue measurements, Global Biogeochemical Cycles, 23, https://doi.org/10.1029/2009GB003523, 2009.

Ostrom, N. E., Pitt, A., Sutka, R., Ostrom, P. H., Grandy, A. S., Huizinga, K. M., and Robertson, G. P.: Isotopologue effects during N_2O reduction in soils and in pure cultures of denitrifiers, Journal of Geophysical Research: Biogeosciences, 112, https://doi.org/10.1029/2006JG000287, 2007.

Pack, A. and Herwartz, D.: The triple oxygen isotope composition of the Earth mantle and understanding $\Delta^{17}O$ variations in terrestrial rocks and minerals, Earth and Planetary Science Letters, 390, 138–145, https://doi.org/10.1016/j.epsl.2014.01.017, 2014.

Sambuichi, T., Tsunogai, U., Kura, K., Nakagawa, F., and Ohba, T.: High-precision $\Delta'^{17}O$ measurements of geothermal H_2O and MORB on the VSMOW-SLAP scale: evidence for active oxygen exchange between the lithosphere and hydrosphere, Geochemical Journal, 55, e25–e33, https://doi.org/10.2343/geochemj.2.0644, 2021.

Sambuichi, T., Tsunogai, U., Ito, M., and Nakagawa, F.: First Measurements on Triple Oxygen Isotopes of Dissolved Inorganic Phosphate in the Hydrosphere, Environmental Science and Technology, 57, 3415–3424, https://doi.org/10.1021/acs.est.2c08520, 2023.

Sharp, Z. D. and Wostbrock, J. A. G.: Standardization for the Triple Oxygen Isotope System: Waters, Silicates, Carbonates, Air, and Sulfates, Reviews in Mineralogy and Geochemistry, 86, 179–196, https://doi.org/10.2138/rmg.2021.86.05, 2021.

Sharp, Z. D., Gibbons, J. A., Maltsev, O., Atudorei, V., Pack, A., Sengupta, S., Shock, E. L., and Knauth, L. P.: A calibration of the triple oxygen isotope fractionation in the

SiO_2–H_2O system and applications to natural samples, Geochimica et Cosmochimica Acta, 186, 105–119, https://doi.org/10.1016/j.gca.2016.04.047, 2016.

Shen, Q. R., Ran, W., and Cao, Z. H.: Mechanisms of nitrite accumulation occurring in soil nitrification, Chemosphere, 50, 747–753, https://doi.org/10.1016/S0045-6535(02)00215-1, 2003.

Snider, D. M., Schiff, S. L., and Spoelstra, J.: $^{15}N/^{14}N$ and $^{18}O/^{16}O$ stable isotope ratios of nitrous oxide produced during denitrification in temperate forest soils, Geochimica et Cosmochimica Acta, 73, 877–888, https://doi.org/10.1016/j.gca.2008.11.004, 2009.

Takahashi, K.: Oxygen isotope ratios between soil water and stem water of trees in pot experiments, Ecological Research, 13, 1–5, https://doi.org/10.1046/j.1440-1703.1998.00240.x, 1998.

Tang, C.-J., Zheng, P., Wang, C.-H., Mahmood, Q., Zhang, J.-Q., Chen, X.-G., Zhang, L., and Chen, J.-W.: Performance of high-loaded ANAMMOX UASB reactors containing granular sludge, Water Research, 45, 135–144, https://doi.org/10.1016/j.watres.2010.08.018, 2011.

Thiemens, M. H. and Trogler, W. C.: Nylon Production: An Unknown Source of Atmospheric Nitrous Oxide, Science, 251, 932–934, https://doi.org/10.1126/science.251.4996.932, 1991.

Tian, H., Xu, R., Canadell, J. G., Thompson, R. L., Winiwarter, W., Suntharalingam, P., Davidson, E. A., Ciais, P., Jackson, R. B., Janssens-Maenhout, G., Prather, M. J., Regnier, P., Pan, N., Pan, S., Peters, G. P., Shi, H., Tubiello, F. N., Zaehle, S., Zhou, F., Arneth, A., Battaglia, G., Berthet, S., Bopp, L., Bouwman, A. F., Buitenhuis, E. T., Chang, J., Chipperfield, M. P., Dangal, S. R. S., Dlugokencky, E., Elkins, J. W., Eyre, B. D., Fu, B., Hall, B., Ito, A., Joos, F., Krummel, P. B., Landolfi, A., Laruelle, G. G., Lauerwald, R., Li, W., Lienert, S., Maavara, T., MacLeod, M., Millet, D. B., Olin, S., Patra, P. K., Prinn, R. G., Raymond, P. A., Ruiz, D. J., van der Werf, G. R., Vuichard, N., Wang, J., Weiss, R. F., Wells, K. C., Wilson, C., Yang, J., and Yao, Y.: A comprehensive quantification of global nitrous oxide sources and sinks, Nature, 586, 248–256, https://doi.org/10.1038/s41586-020-2780-0, 2020.

Toyoda, S., Yano, M., Nishimura, S., Akiyama, H., Hayakawa, A., Koba, K., Sudo, S., Yagi, K., Makabe, A., Tobari, Y., Ogawa, N. O., Ohkouchi, N., Yamada, K., and Yoshida, N.: Characterization and production and consumption processes of N_2O emitted from temperate agricultural soils determined via isotopomer ratio analysis, Global Biogeochemical Cycles, 25, https://doi.org/10.1029/2009GB003769, 2011.

Toyoda, S., Kuroki, N., Yoshida, N., Ishijima, K., Tohjima, Y., and Machida, T.: Decadal time series of tropospheric abundance of N_2O isotopomers and isotopologues in the Northern Hemisphere obtained by the long-term observation at Hateruma Island, Japan,

设置了格式：字体颜色：黑色

Journal of Geophysical Research: Atmospheres, 118, 3369–3381, https://doi.org/10.1002/jgrd.50221, 2013.

Toyoda, S., Yoshida, N., and Koba, K.: Isotopocule analysis of biologically produced nitrous oxide in various environments, Mass Spectrometry Reviews, 36, 135–160, https://doi.org/10.1002/mas.21459, 2017.

Tsunogai, U., Ishibashi, J., Wakita, H., and Gamo, T.: Methane-rich plumes in the Suruga Trough (Japan) and their carbon isotopic characterization, Earth and Planetary Science Letters, 160, 97–105, https://doi.org/10.1016/S0012-821X(98)00075-2, 1998.

Tsunogai, U., Hachisu, Y., Komatsu, D. D., Nakagawa, F., Gamo, T., and Akiyama, K.: An updated estimation of the stable carbon and oxygen isotopic compositions of automobile CO emissions, Atmospheric Environment, 37, 4901–4910, https://doi.org/10.1016/j.atmosenv.2003.08.008, 2003.

Tsunogai, U., Kido, T., Hirota, A., Ohkubo, S. B., Komatsu, D. D., and Nakagawa, F.: Sensitive determinations of stable nitrogen isotopic composition of organic nitrogen through chemical conversion into N_2O, Rapid Communications in Mass Spectrometry, 22, 345–354, https://doi.org/10.1002/rcm.3368, 2008.

Tsunogai, U., Komatsu, D. D., Daita, S., Kazemi, G. A., Nakagawa, F., Noguchi, I., and Zhang, J.: Tracing the fate of atmospheric nitrate deposited onto a forest ecosystem in Eastern Asia using $\Delta^{17}O$, Atmospheric Chemistry and Physics, 10, 1809–1820, https://doi.org/10.5194/acp-10-1809-2010, 2010.

Tsunogai, U., Kamimura, K., Anzai, S., Nakagawa, F., and Komatsu, D. D.: Hydrogen isotopes in volcanic plumes: Tracers for remote temperature sensing of fumaroles, Geochimica et Cosmochimica Acta, 75, 4531–4546, https://doi.org/10.1016/j.gca.2011.05.023, 2011.

Tsushima, I., Ogasawara, Y., Kindaichi, T., Satoh, H., and Okabe, S.: Development of high-rate anaerobic ammonium-oxidizing (anammox) biofilm reactors, Water Research, 41, 1623–1634, https://doi.org/10.1016/j.watres.2007.01.050, 2007.

Uechi, Y. and Uemura, R.: Dominant influence of the humidity in the moisture source region on the ^{17}O-excess in precipitation on a subtropical island, Earth and Planetary Science Letters, 513, 20–28, https://doi.org/10.1016/j.epsl.2019.02.012, 2019.

Verhoeven, E., Barthel, M., Yu, L., Celi, L., Said-Pullicino, D., Sleutel, S., Lewicka-Szczebak, D., Six, J., and Decock, C.: Early season N_2O emissions under variable water management in rice systems: source-partitioning emissions using isotope ratios along a depth profile, Biogeosciences, 16, 383–408, https://doi.org/10.5194/bg-16-383-2019, 2019.

Wankel, S. D., Ziebis, W., Buchwald, C., Charoenpong, C., de Beer, D., Dentinger, J., Xu, Z., and Zengler, K.: Evidence for fungal and chemodenitrification based N_2O flux

from nitrogen impacted coastal sediments, Nature Communication, 8, 15595, https://doi.org/10.1038/ncomms15595, 2017.

WMO.: WMO greenhouse gas bulletin (GHG Bulletin), Assessed from: https://library.wmo.int/records/item/68532-no-19-15-november-2023, 2023.

Wrage, N., Velthof, G. L., van Beusichem, M. L., and Oenema, O.: Role of nitrifier denitrification in the production of nitrous oxide, Soil Biology and Biochemistry, 33, 1723–1732, https://doi.org/10.1016/S0038-0717(01)00096-7, 2001.

Wrage, N., Lauf, J., del Prado, A., Pinto, M., Pietrzak, S., Yamulki, S., Oenema, O., and Gebauer, G.: Distinguishing sources of N_2O in European grasslands by stable isotope analysis, Rapid Communications in Mass Spectrometry, 18, 1201–1207, https://doi.org/10.1002/rcm.1461, 2004.

Wrage, N., Groenigen, J. W. van, Oenema, O., and Baggs, E. M.: A novel dual-isotope labelling method for distinguishing between soil sources of N_2O, Rapid Communications in Mass Spectrometry, 19, 3298–3306, https://doi.org/10.1002/rcm.2191, 2005.

Xu, H., Tsunogai, U., Nakagawa, F., Li, Y., Ito, M., Sato, K., and Tanimoto, H.: Determination of the triple oxygen isotopic composition of tropospheric ozone in terminal positions using a multistep nitrite-coated filter-pack system, Rapid Communications in Mass Spectrometry, 35, e9124, https://doi.org/10.1002/rcm.9124, 2021.

Yan, Y., Sha, L., Cao, M., Zheng, Z., Tang, J., Wang, Y., Zhang, Y., Wang, R., Liu, G., Wang, Y., and Sun, Y.: Fluxes of CH_4 and N_2O from soil under a tropical seasonal rain forest in Xishuangbanna, Southwest China, Journal of Environmental Sciences, 20, 207–215, https://doi.org/10.1016/S1001-0742(08)60033-9, 2008.

York, D., Evensen, N. M., Martínez, M. L., and De Basabe Delgado, J.: Unified equations for the slope, intercept, and standard errors of the best straight line, American Journal of Physics, 72, 367–375, https://doi.org/10.1119/1.1632486, 2004.

Young, E. D., Galy, A., and Nagahara, H.: Kinetic and equilibrium mass-dependent isotope fractionation laws in nature and their geochemical and cosmochemical significance, Geochimica et Cosmochimica Acta, 66, 1095–1104, https://doi.org/10.1016/S0016-7037(01)00832-8, 2002.

Yu, L., Harris, E., Lewicka-Szczebak, D., Barthel, M., Blomberg, M. R. A., Harris, S. J., Johnson, M. S., Lehmann, M. F., Liisberg, J., Müller, C., Ostrom, N. E., Six, J., Toyoda, S., Yoshida, N., and Mohn, J.: What can we learn from N_2O isotope data? – Analytics,

processes and modelling, Rapid Communications in Mass Spectrometry, 34, e8858, https://doi.org/10.1002/rcm.8858, 2020.

Zhang, W., Li, Y., Xu, C., Li, Q., and Lin, W.: Isotope signatures of N_2O emitted from vegetable soil: Ammonia oxidation drives N_2O production in NH_4^+-fertilized soil of North China, *Scientific Reports*, 6, 29257, https://doi.org/10.1038/srep29257, 2016.

Zhu, G., Wang, S., Wang, Y., Wang, C., Risgaard-Petersen, N., Jetten, M. S., and Yin, C.: Anaerobic ammonia oxidation in a fertilized paddy soil, ISME Journal, 5, 1905–1912, https://doi.org/10.1038/ismej.2011.63, 2011.

Zhu, X., Burger, M., Doane, T. A., and Horwath, W. R.: Ammonia oxidation pathways and nitrifier denitrification are significant sources of N_2O and NO under low oxygen availability, Proceedings of the National Academy of Sciences, 110, 6328–6333, https://doi.org/10.1073/pnas.1219993110, 2013.

Zou, Y., Hirono, Y., Yanai, Y., Hattori, S., Toyoda, S., and Yoshida, N.: Rainwater, soil water, and soil nitrate effects on oxygen isotope ratios of nitrous oxide produced in a green tea (*Camellia sinensis*) field in Japan, Rapid Communications in Mass Spectrometry, 29, 891–900, https://doi.org/10.1002/rcm.7176, 2015.

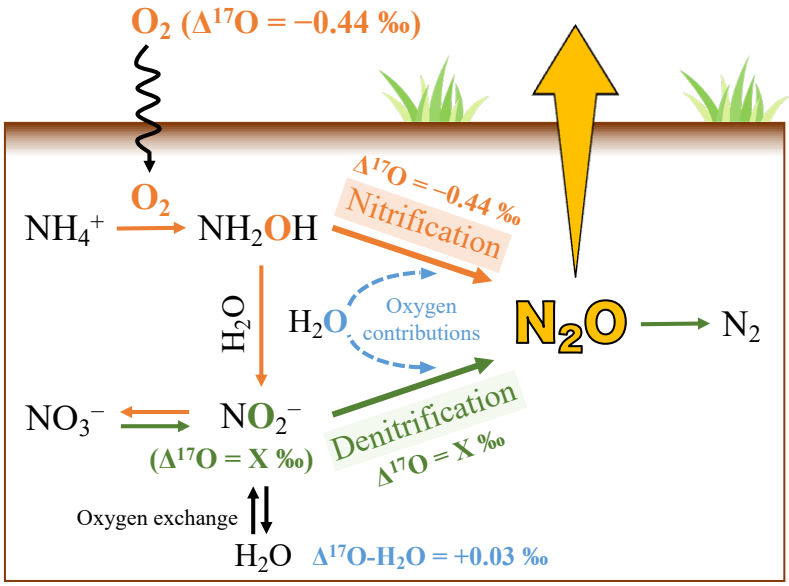

953 **Figure 1.** Schematic showing the pathways of N_2O production in soil (Kool et al., 2007,
954 2011; Wankel et al., 2017; Wrage et al., 2005) and the $\Delta^{17}O$ values of O_2 (Sharp et al.,
955 2016), NO_2^-, and H_2O (Uechi and Uemura, 2019). The orange lines, green lines, and blue
956 dash lines indicate the processes of nitrification, denitrification, and the possible
957 contributions of O atoms derived from soil H_2O through nitrification and denitrification,
958 respectively.
959

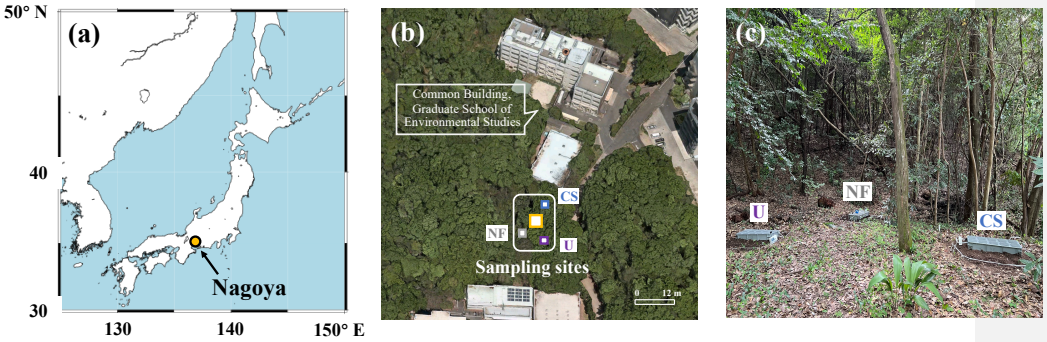

960 **Figure 2.** Map showing the location of Nagoya, Japan, where the studied site is located
961 (a). Map showing the monitoring site of N_2O emitted from forested soil in a secondary
962 warm-temperate forest (yellow square) and the plots fertilized with Chile saltpeter (CS,
963 blue square), urea (U, purple square), and no fertilizer (NF, gray square) (b). Photo
964 showing the plots and flow chambers set on the plots (c).
965

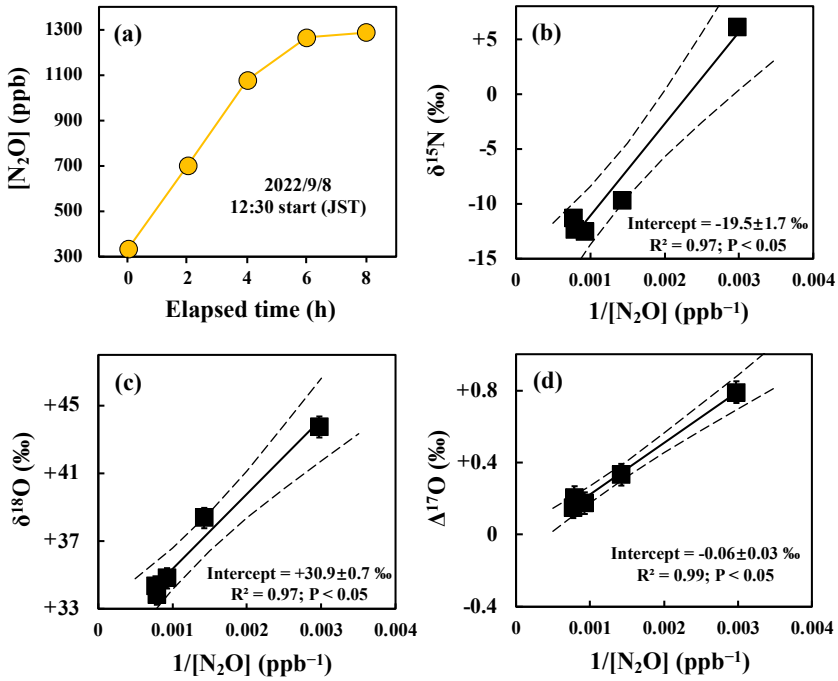

966 **Figure 3.** An example of changes in the concentration of N_2O ([N_2O]) in gas samples
967 during the observation on September 8, 2022, plotted as a function of the elapsed time
968 since the deployment of the flow chamber on the forested soil (a), and the $\delta^{15}N$ (b), $\delta^{18}O$
969 (c), and $\Delta^{17}O$ (d) values of N_2O plotted as a function of the reciprocal of [N_2O] (1/[N_2O])
970 during the observation. Each solid line is the least squares fitting of the samples, while
971 each dotted line is the 2σ confidence interval of the fitting line. Error bars smaller than
972 the sizes of the symbols are not shown.

973

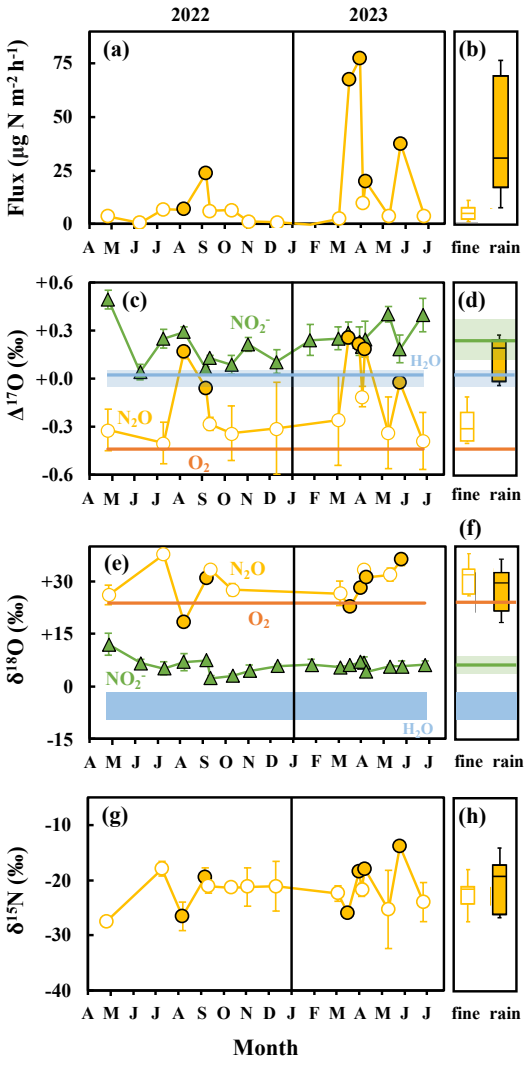

974 **Figure 4.** Temporal variations in the flux (a), $\Delta^{17}O$ (c), $\delta^{18}O$ (e), and $\delta^{15}N$ (g) values of
975 N_2O emitted from the forested soil, and the $\delta^{18}O$ and $\Delta^{17}O$ values of soil NO_2^- (green
976 triangles), O_2 (orange lines), and soil H_2O (blue area or line). Sampling performed on fine
977 and rainy days is indicated by the open (white) and solid (yellow) circles, respectively,

with the box plots of the emission flux (b), $\Delta^{17}O$ (d), $\delta^{18}O$ (f), and $\delta^{15}N$ (h) of N_2O on fine and rainy days. The black lines of the box plots indicate the median values. The lower and upper boundaries of the box plots indicate the lower (25 %) and upper (75 %) quartiles of data for each component, respectively. The whiskers of the box plots denote the entire range of values for each component. Error bars smaller than the sizes of the symbols are not shown.

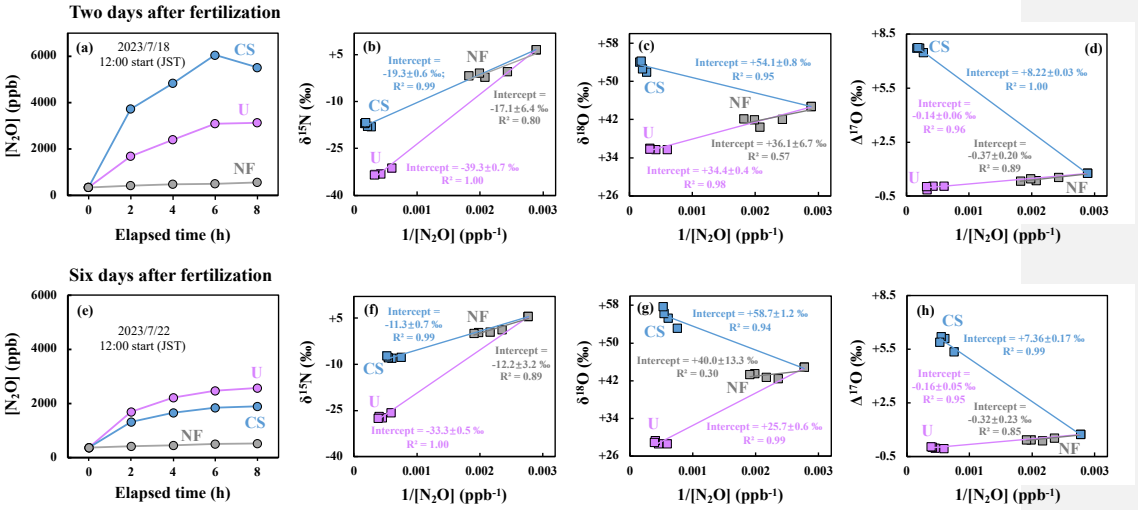

Figure 5. Changes in $[N_2O]$ of gas samples collected from the plots of NF (gray), U (purple), and CS (blue) 2 days after fertilization (a) and 6 days after fertilization (e) and plotted as a function of the elapsed time since the deployment of the flow chamber; the $\delta^{15}N$ (b and f), $\delta^{18}O$ (c and g), and $\Delta^{17}O$ (d and h) values of N_2O plotted as a function of the reciprocal of $[N_2O]$ ($1/[N_2O]$). Error bars smaller than the sizes of the symbols are not shown.

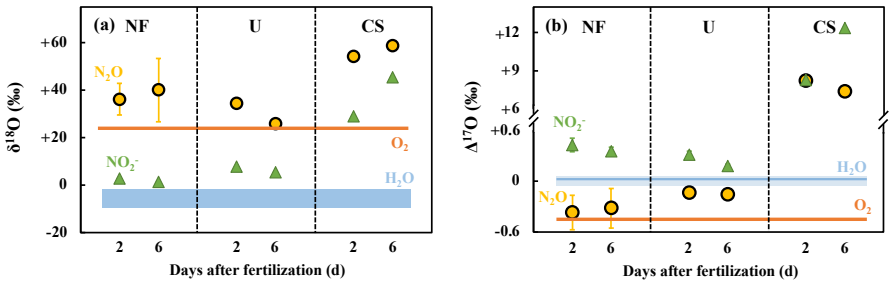

992 **Figure 6.** The $\delta^{18}O$ (a) and $\Delta^{17}O$ (b) values of N_2O (yellow circles) and NO_2^- (green
993 triangles) in NF, U, and CS plots determined 2 and 6 days after fertilization, and the $\delta^{18}O$
994 and $\Delta^{17}O$ values of O_2 (orange lines) and soil H_2O (blue area or line). Error bars smaller
995 than the sizes of the symbols are not shown.

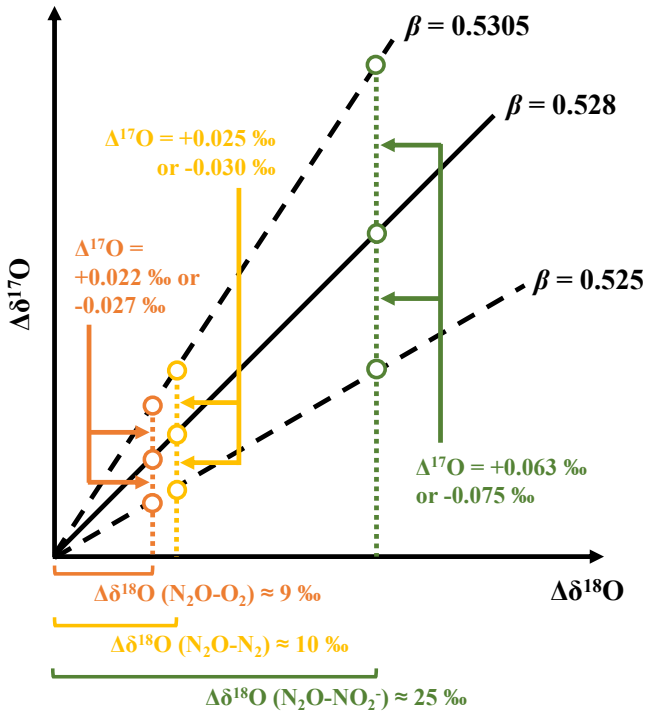

996 **Figure 7.** Schematic showing the possible variations in the $\Delta^{17}O$ value of N_2O from that
997 of the source of O atoms (O_2 and NO_2^-) during transformations, including nitrification
998 (orange circles), denitrification (green circles), and reduction (yellow circles), due to
999 variations in isotope fractionation and β from 0.525 to 0.5305.